Hydrogen Peroxide Clusters: The Role of Open Book Motif in Cage and Helical Structures

M. Elango, R. Parthasarathi, and V. Subramanian*

Chemical Laboratory, Central Leather Research Institute, Adyar, Chennai, India 600 020

C. N. Ramachandran and N. Sathyamurthy*

Department of Chemistry, Indian Institute of Technology Kanpur, Kanpur, India 208 016

Received: October 12, 2005; In Final Form: March 22, 2006

Hartree−Fock (HF) calculations using 6-31G*, 6-311++G(d,p), aug-cc-pVDZ, and aug-cc-pVTZ basis sets show that hydrogen peroxide molecular clusters tend to form hydrogen-bonded cyclic and cage structures along the lines expected of a molecule which can act as a proton donor as well as an acceptor. These results are reiterated by density functional theoretic (DFT) calculations with B3LYP parametrization and also by second-order Møller−Plesset perturbation (MP2) theory using 6-31G* and 6-311++G(d,p) basis sets. Trends in stabilization energies and geometrical parameters obtained at the HF level using 6-311++G(d,p), aug-cc-pVDZ, and aug-cc-pVTZ basis sets are similar to those obtained from HF/6-31G* calculation. In addition, the HF calculations suggest the formation of stable helical structures for larger clusters, provided the neighbors form an open book structure.

I. Introduction

Hydrogen-bonded molecular clusters have been studied extensively over the years because of their importance in physics, chemistry, and biology.[1,2] The water dimer is a classic example used to illustrate hydrogen-bonding interaction. The amount of literature available on the dimer and larger clusters of water molecules is enormous (for examples, see ref 3 and references therein). While the water dimer is known to form a linear structure with a single hydrogen bond, the trimer prefers a cyclic arrangement in which each water molecule acts as a hydrogen donor as well as an acceptor. The tetramer and the pentamer also seem to prefer cyclic structures. The transition from two-dimensional structures to three-dimensional structures occurs for $(H_2O)_n$, at $n = 6$.[4] Detailed quantum calculations show that the water hexamer has a number of conformers such as ring, nonplanar open book, closed cage, and prism that are close in energy.[5] While early experiments suggested a cage structure at 5 K, more recent experiments suggest that the open book structure is preferred at cluster temperatures between 50 and 60 K.[4,6]

One of the closest relatives of water is hydrogen peroxide (HP). The monomer of the latter is a textbook example of a small molecule exhibiting a nonplanar open book structure. It is also perhaps the smallest chiral molecule, which can donate a proton and also accept a proton. Although HP is a highly reactive species, its dimer has been studied experimentally using matrix isolation spectroscopy[7] and compared with the theoretical predictions. Extensive ab initio calculations have been carried out for the trimer and the tetramer also recently.[8] It has been shown that HP forms a cyclic dimer and that the structure with two non-hydrogen-bonded O−H bonds pointing away from each other (**2-UD**, **U** = up, **D** = down) is slightly more stable than the one (**2-UU**) with both the hydrogens pointing in the same side of the O−O−O−O plane. The trimer and the tetramer were also shown to form closed cyclic structures, with the tetramer being clearly nonplanar. To the best of our knowledge, there has been no other report on HP clusters. Therefore, a systematic investigation of $(HP)_n$ clusters, where $n = 1-15$, 22, and 28, has been undertaken using different quantum mechanical methods. It is shown that the hydrogen peroxide trimer (**3A**) structure plays an important role in building larger clusters and that it acts as a structural motif in building helical structures.

II. Computational Methodology

Optimized geometries of HP and its clusters $(HP)_n$, $n = 2-15$, 22, and 28, have been obtained without imposing any constraints at different levels of theory [Hartree−Fock (HF), density functional theory (DFT) using B3LYP parametrization, and Møller−Plesset second-order perturbation (MP2) theory] with a manageable basis set 6-31G* using the *Gaussian 98W* suite of programs.[9] Our past experience has shown that such a basis set leads to the right conclusion regarding the structure and relative stability of hydrogen-bonded molecular clusters,[3,10,11] even if it does not lead to quantitatively correct stabilization energies. Effect of larger basis sets on the stabilization energies and geometrical parameters has also been probed using 6-311++G(d,p), aug-cc-pVDZ, and aug-cc-pVTZ basis sets at the HF level. Stabilization energies (SEs) of all the clusters have been calculated using the supermolecule approach

$$\mathrm{SE} = -(E_{\mathrm{cluster}} - E_{\mathrm{monomers}}) \qquad (1)$$

where E_{cluster} and E_{monomers} refer to the energies of the cluster and the monomers, respectively. The results have been corrected for basis set superposition error (BSSE) following the procedure adopted by Boys and Bernardi.[12] Stabilization energies for the $(HP)_n$ clusters, where $n = 2-15$, were also corrected for zero-point energy (ZPE). To ensure that the optimized geometries correspond to true minima in energy space, vibrational frequencies were computed by the HF method for all the $(HP)_n$ clusters

* Authors for correspondence. E-mail: subuchem@hotmail.com; nsath@iitk.ac.in. Tel: +91 44 24411630; +91 512 2597390/2597367. Fax: +91 44 24911589; +91 512 2597390.

10.1021/jp055818r CCC: $33.50
Published on Web 04/25/2006

TABLE 1: Geometrical Parameters and Relative Stabilities of Various Conformers of Hydrogen Peroxide Calculated at Various Levels of Theory[a]

	relative stability[a] (kcal/mol)			geometries of open book structure			
level	a	b	c	O−H (Å)	O−O (Å)	O−O−H (°)	H−O−O−H (°)
HF/6-31G*	0.0	9.2	0.9	0.949	1.396	102.1	116.0
HF/6-311++G(d,p)	0.0	8.6	0.9	0.943	1.385	102.9	117.6
HF/aug-cc-pVDZ	0.0	7.5	1.2	0.943	1.387	103.1	111.6
HF/aug-cc-pVTZ	0.0	7.8	1.2	0.945	1.389	102.8	111.2
B3LYP/6-31G*	0.0	8.9	0.7	0.973	1.455	99.7	118.7
MP2/6-31G*	0.0	9.4	0.6	0.975	1.468	98.6	121.3
MP2/6-311++G(d,p)	0.0	9.0	1.0	0.965	1.450	99.6	121.5
experimental[17]				0.965	1.464	99.4	111.8

[a] Refer to Figure 1 for definition of a, b, and c.

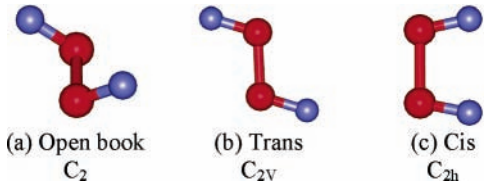

Figure 1. Different conformers of hydrogen peroxide, along with the point group classification. Large spheres represent the oxygen atoms and small spheres the hydrogen atoms.

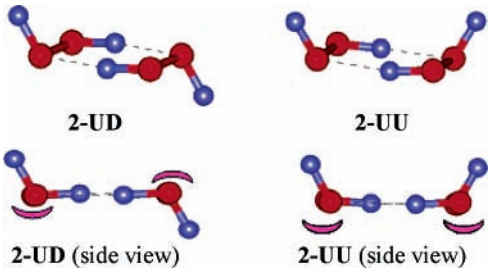

Figure 2. Two different conformers of hydrogen peroxide dimer.

studied except $n = 22$ and 28. The vibrational frequencies were scaled[13] by a factor of 0.8929 for comparison with experiment wherever applicable. The theory of atoms-in-molecules (AIM) has been used to characterize the hydrogen-bonding interaction using topological properties of the electron density at the hydrogen bond critical points (HBCPs) using the *AIM2000* package.[14] In addition, molecular electrostatic potential (MESP) maps[15] of various clusters have been generated using *GaussView 3.0* software package.[16]

III. Results and Discussion

Although the open book structure of HP is well-known, it was investigated through ab initio calculations to provide the basis for further work in the present study. The calculated H−O and O−O bond lengths, the H−O−O bond angle, and the torsion angle along with the experimental values are listed in Table 1. The optimized structures of various conformers of HP are provided in Figure 1. It could be seen from Table 1 that the DFT and MP2 results are in better agreement with experiment than the HF results. MP2/6-31G* calculations show the planar cis and trans conformations to be less stable than the most stable nonplanar open book structure by 9.4 and 0.6 kcal/mol, respectively. It is found from the larger basis set calculations that there are no significant changes in the geometrical parameters when compared to those obtained from HF/6-31G* calculations. Not surprisingly, the relative energies predicted by the larger basis set calculations do differ slightly from the HF/6-31G* results. However, the open book structure is found to be the most stable conformer as predicted by HF/6-31G* calculations.

TABLE 2: Dipole Moments, Geometrical Parameters, and Relative Energies of Two Conformers of Hydrogen Peroxide Dimer Calculated at Various Levels of Theory

	dipole moment (Debye)		relative energy (kcal/mol)		O−O−O−O dihedral angle (°)	
level	**2-UU**	**2-UD**	**2-UU**	**2-UD**	**2-UU**	**2-UD**
HF/6-31G*	3.4	0.0	0.5	0.0	26.2	0.0
HF/6-311++G(d,p)	3.4	0.0	0.1	0.0	33.9	0.0
HF/aug-cc-pVDZ	3.3	0.0	0.1	0.0	35.2	0.0
HF/aug-cc-pVTZ	3.3	0.0	0.1	0.0	35.0	0.0
B3LYP/6-31G*	2.9	0.0	0.6	0.0	3.6	0.0
MP2/6-31G*	3.1	0.0	0.6	0.0	2.9	0.0
MP2/6-311++G(d,p)	3.4	0.0	0.2	0.0	24.3	0.0

Two cyclic conformations for the HP dimer are illustrated in Figure 2. As reported by Kulkarni et al.,[8] the dimer has two energetically close conformers denoted **2-UD** and **2-UU**. The position of the lone pairs on the oxygen atoms of the dimers is also indicated in Figure 2. It is clear that the lone pairs are on one side of the O−O−O−O plane in **2-UU** and on opposite sides in the **2-UD** conformation. As reported by those authors, the **2-UD** conformation is slightly more stable than the **2-UU** by 0.5−0.6 kcal/mol at HF, DFT (B3LYP), and MP2 levels of theory (Table 2). Larger basis set calculations at the HF level also reaffirmed that the **UD** conformer is more stable than **UU**. The dipole moment of **2-UD** is 0, whereas that of **2-UU** is 3.4 D at the HF/6-31G* level of calculation. HF/aug-cc-pVDZ, HF/aug-cc-pVTZ, HF/6-311++G(d,p), B3LYP/6-31G*, MP2/6-311++G(d,p), and MP2/6-31G* calculations predict comparable dipole moments for **2-UU**.

The HP trimer has different possible conformations such as open linear, cyclic, and prism structures. The optimized geometries as obtained from HF/6-31G* calculations are

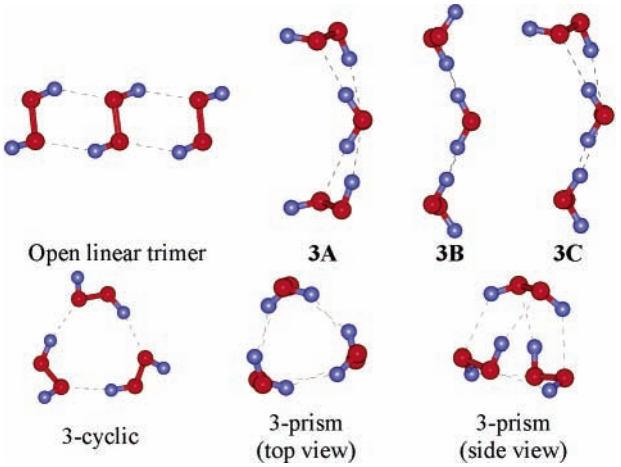

Figure 3. Optimized geometries of linear, cyclic, and three-dimensional structures of hydrogen peroxide trimer obtained from HF calculations.

TABLE 3: Stabilization Energies (SE in kcal/mol) for Different Conformers of $(HP)_n$ Clusters[a]

	6-31G*				aug-cc-pVDZ				aug-cc-pVTZ			
cluster	SE	BSSE corrected	ZPE correction	BSSE + ZPE corrected	SE	BSSE corrected	ZPE correction	BSSE + ZPE corrected	SE	BSSE corrected	ZPE correction	BSSE + ZPE corrected
2-UD	8.2	6.7	2.0	4.7	6.1	5.6	2.0	3.6	5.6	5.4	1.9	3.6
2-UU	7.7	6.4	2.0	4.4	5.9	5.4	2.0	3.5	5.4	5.3	1.9	3.4
3A	15.9	13.3	3.7	9.6	12.3	11.3	3.8	7.5	12.1	11.3	3.6	8.5
3B	16.6	13.7	3.8	9.9	12.4	11.4	3.7	7.7	12.2	11.3	3.7	8.6
3C	16.6	13.8	3.9	9.9	12.6	11.6	3.9	7.7	12.3	11.5	3.7	8.6
3-cyclic	15.4	13.3	3.0	10.3	12.1	11.2	3.0	8.2	12.3	11.4	3.4	9.3
3-prism	15.4	9.6	4.3	5.3	9.9	8.3	3.8	4.5	8.9	8.2	3.0	5.5
4	24.2	20.4	5.6	14.8	18.9	17.2	5.6	11.6				
4-cyclic	27.9	21.0	6.9	14.1	19.9	17.5	6.6	10.9				
5	32.7	27.5	5.5	22.0	25.5	23.2	7.5	15.8				
5-cyclic	37.9	30.7	10.6	20.1	28.0	25.6	8.7	17.0				
6	41.1	34.6	9.2	25.4	32.0	29.2						
6-cage-1	44.5	32.3	10.3	22.0	30.7	27.1						
6-cage-2	43.9	32.9	10.1	22.8	30.7	27.4						

[a] Where $n = 2-6$, calculated by HF method using different basis sets and corrected for BSSE and zero-point energy (ZPE).

TABLE 4: Stabilization Energies (SE in kcal/mol) for Different Conformers of $(HP)_n$ Clusters[a]

	HF/6-31G*		DFT(B3LYP)/6-31G*		MP2/6-31G*	
cluster	SE	BSSE corrected	SE	BSSE corrected	SE	BSSE corrected
2-UD	8.2	6.7	12.0	9.2	11.8	8.3
2-UU	7.7	6.4	11.4	8.5	11.2	7.7
3A	15.9	13.3	23.8	18.1	21.4	16.3
3B	16.6	13.7	24.9	19.4	24.6	17.5
3C	16.6	13.8	25.0	20.6	24.5	17.3
3-cyclic	15.4	13.3	27.7	17.9	27.2	16.1
3-prism	15.4	9.6	21.1	15.8	27.2	13.7
4	24.2	20.4	4-cyclic	4-cyclic	4-cyclic	4-cyclic
4-cyclic	27.9	21.0	47.8	33.9	46.7	29.7
5	32.7	27.5	5-cyclic	5-cyclic	5-cyclic	5-cyclic
5-cyclic	37.9	30.7	62.5	47.8	61.3	42.4
6	41.1	34.6	6-cage-2	6-cage-2	6-cage-2	6-cage-2
6-cage-1	44.5	32.3	75.0	51.4	72.7	44.0
6-cage-2	43.9	32.9	73.8	51.9	71.1	43.8
7	49.4	41.6	7-cage	7-cage		
7-cage	56.3	44.9	90.9	65.9		
8	57.8	48.7	8-cage-2	8-cage-2		
8-cage-1	68.3	53.7	111.1	83.1		
8-cage-2	67.4	53.6	106.5	79.7		
9	66.1	55.7	9-cage	9-cage		
9-cage	77.5	63.6	120.8	92.8		
10	74.5	62.8	109.8	87.2		
10-cage	87.7	71.0	140.3	108.0		
11	82.8	69.8	122.1	97.1		
12	91.2	77.0	134.4	106.9		
12-cage	104.7	85.3	132.6	114.8		
13	99.5	84.0	146.7	116.7		
14	107.9	91.0	159.0	126.5		
15	116.2	98.1	171.3	136.5		
22	174.7	147.5	257.5	205.4		
28	224.8	189.8	331.3	246.6		

[a] Where $n = 2-15$, 22, and 28, calculated by different methods using the basis set 6-31G* and corrected for basis set superposition error (BSSE). Whenever the geometry optimization results in another geometry, the same is indicated.

TABLE 5: Stabilization Energies (SE in kcal/mol) for Different Conformers of $(HP)_n$ Clusters[a]

	HF		MP2	
cluster	BSSE uncorrected	BSSE corrected	BSSE uncorrected	BSSE corrected
2-UD	6.9	6.0	9.4	6.8
2-UU	6.7	5.9	9.2	6.6
3A	14.0	12.4	19.5	14.0
3B	14.0	12.4	19.7	14.3
3C	14.2	12.5	19.9	14.4
3-cyclic	14.1	12.6	18.8	13.5
3-prism	10.7	8.6	17.5	11.7
4	21.4	18.8	4-cyclic	4-cyclic
4-cyclic	21.7	18.4	34.1	24.0
5	28.9	25.4	5-cyclic	5-cyclic
5-cyclic	31.0	27.2	48.3	34.2
6	36.3	32.6	6-cage-2	6-cage-2
6-cage-1	34.1	29.0	55.8	37.1
6-cage-2	34.3	29.4	53.6	35.7
7	43.7	41.0		
7-cage	50.7	46.5		
8	51.1	47.8		
8-cage-1	55.6	51.1		
8-cage-2	56.6	52.1		
9	58.5	54.7		
9-cage	68.2	62.9		
10	65.9	61.6		
10-cage	72.9	67.4		
11	73.3	68.4		
12	80.7	78.6		
12-cage	87.0	80.7		
13	88.1	103.9		
14	95.5	112.4		
15	102.9	121.0		
22	154.7	180.7		
28	199.1	232.0		

[a] Where $n = 2-15$, 22, and 28, calculated by HF and MP2 methods using the basis set 6-311++G(d,p) and corrected for basis set superposition error (BSSE).

presented in Figure 3. Although the cyclic structure was reported in an earlier investigation,[8] two new stable conformations have been predicted in the present study. The open structure is predicted to be more stable than the 3-prism structure by 3.7, 2.3, and 2.6 kcal/mol by HF/6-31G*, DFT (B3LYP)/6-31G*, and MP2/6-31G* calculations. HF calculations using 6-311++G-(d,p), aug-cc-pVDZ, and aug-cc-pVTZ basis sets for the trimers reveal that the cyclic conformer is the most stable, followed by open and prism structures. However, there is no significant change in the geometrical parameters in going from one basis set to another. It is important to note from Tables 3−5 that the difference in stabilization energy between the most stable cyclic structure and the open structures is within 1 kcal/mol. Both **2-UU** and **2-UD** conformers have been used to construct three different structures (**3A**, **3B**, and **3C**) in the open linear configuration for the trimer. The planes containing the four oxygen atoms of two adjacent HP molecules are at 30° with respect to each other in **3A**, which leads to self-curling. Curling in the other two structures, **3B** and **3C**, is much less. In **3A**, the

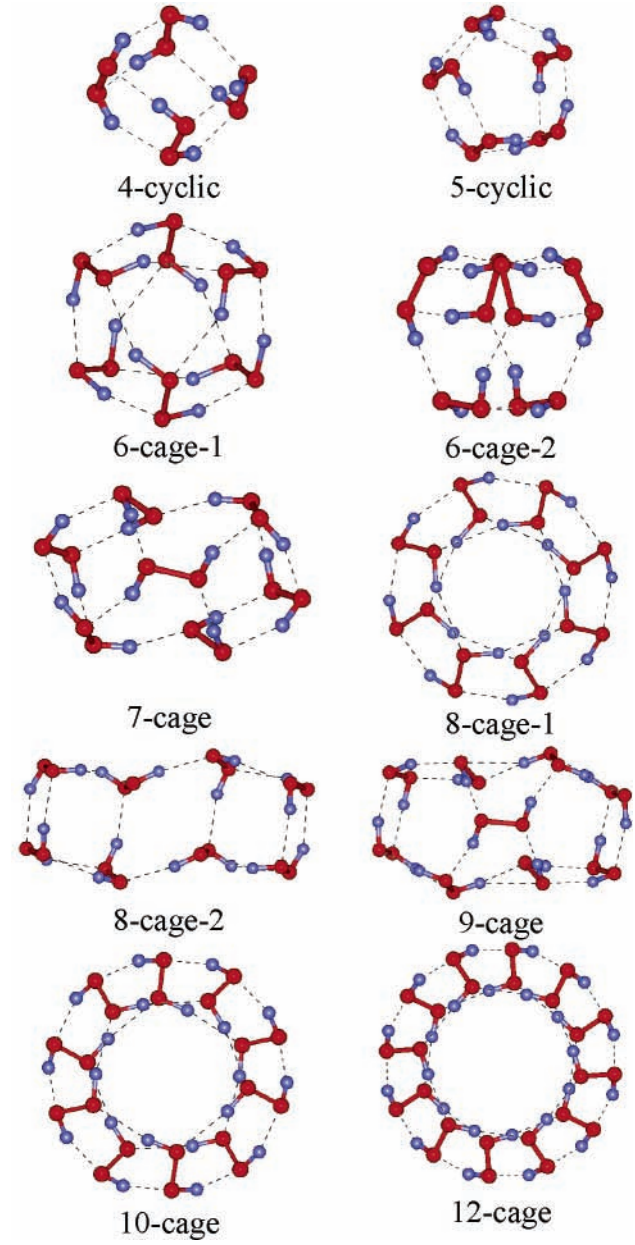

Figure 4. Optimized geometries of cyclic and cage-shaped hydrogen peroxide clusters as obtained from HF calculations.

lone pairs on all the oxygen atoms are on the same side of the plane, whereas in the other two structures, this is not the case. It is important to note that the structure **3A** is similar to the open book structure observed for the water hexamer.

With the **3A** structure as the starting arrangement, more HP molecules were added to construct open as well as closed clusters as illustrated in Figures 4 and 5. The tetramer has a cubic configuration as the most stable geometry in which all eight hydrogen atoms are involved in hydrogen bonding. Similar to the tetramer, the pentamer also exhibits a cyclic structure wherein all the hydrogen atoms participate in the formation of hydrogen bonds. Various cyclic and cage structures of larger $(HP)_n$ clusters up to $n = 12$ determined in this study are displayed in Figure 4. The stabilization energies of these structures are listed in Tables 3−5.

Curling in the tetramer and the larger clusters suggests the possibility of constructing helical motifs by adding more HP moieties. Hence, the possibility of formation of helical structures in larger clusters has been investigated using HF calculations.

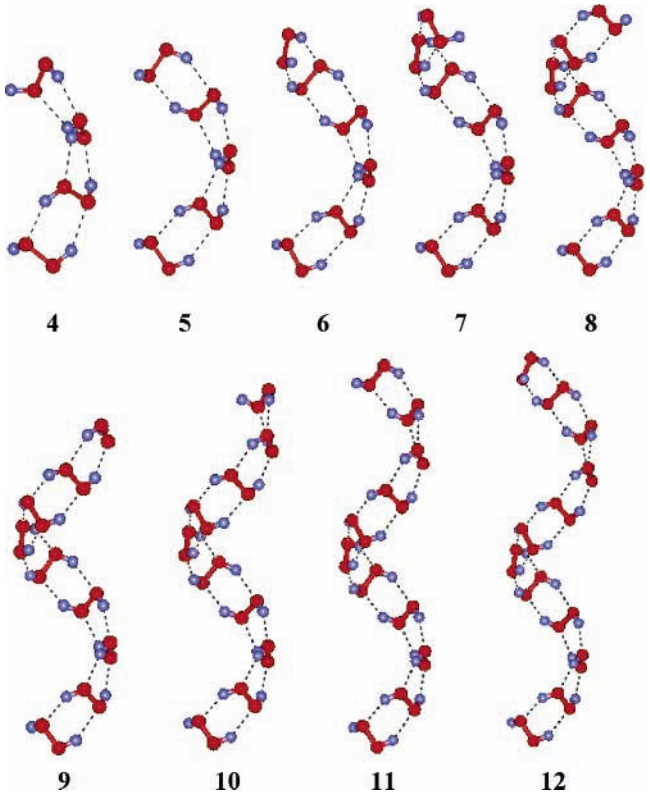

Figure 5. Optimized geometries of open linear helical structures of $(HP)_n$ clusters, where $n = 4-12$ obtained from HF calculations.

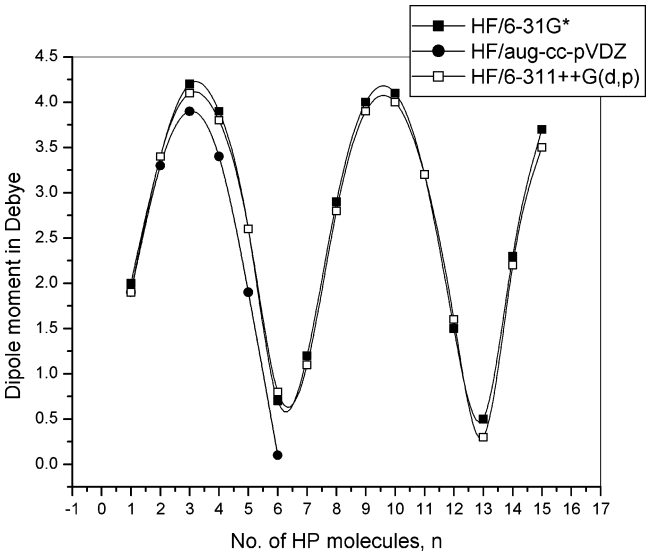

Figure 6. Variation of dipole moment with the number (n) of hydrogen peroxide molecules in the helical structure as obtained from HF calculations using different basis sets.

The resulting optimized geometries for $(HP)_n$, $n \leq 12$, are shown in Figure 5, and their stabilization energies are reported in Tables 3−5. It is important to point out here that all the HP molecules exhibit open book conformation in the helical structure. As can be seen from Tables 3−5, the addition of each HP molecule increases the stability of the helical structure. For $(HP)_{13}$, the stabilization energy is 84.0 kcal/mol, and for $(HP)_{28}$, it is 189.6 kcal/mol. The stabilization energy per hydrogen bond for the **2-UD** dimer is 3.35 kcal/mol, and for $(HP)_{28}$, it is 3.5 kcal/mol, thus clearly illustrating that there is no dramatic change in hydrogen bonding between two adjacent HP molecules in the larger helical structures.

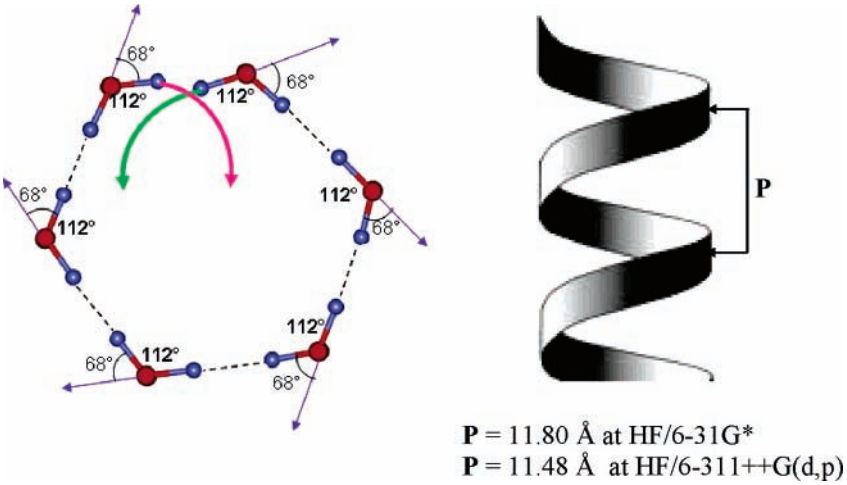

Figure 7. Schematic representation of the helix formation and the calculated pitch (*P*) of the helix for $n = 28$ cluster.

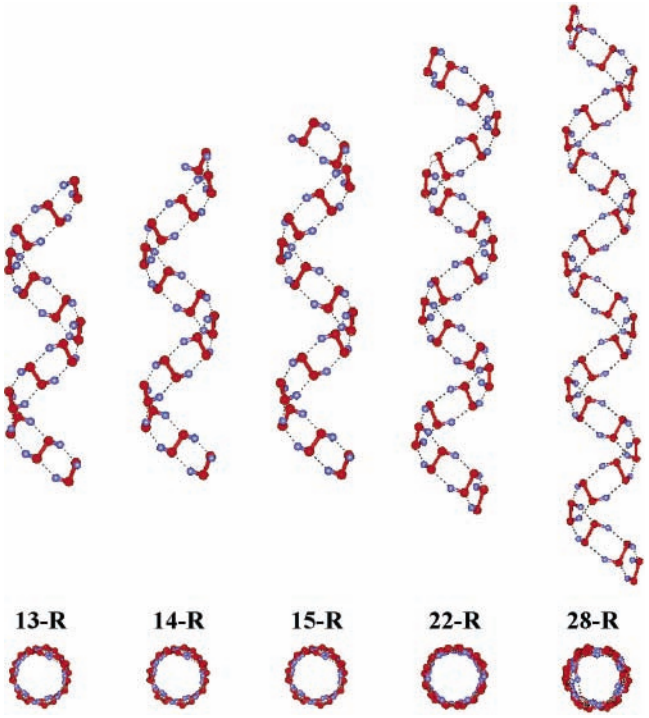

Figure 8. Optimized geometries of helical structures of hydrogen peroxide clusters obtained from HF calculations. Top views are provided at the bottom.

The dipole moment of the peptide bond is known to play a crucial role in the stabilization of the α-helical structure. A spiral structure based on dipole−dipole electrostatic interactions has been proposed for negatively charged large clusters of N-monosubstituted amide molecules recently.[18] To analyze the importance of dipole moment in the formation of the helical structure in $(HP)_n$ clusters, the variation of the dipole moment with *n*, as computed from HF calculations, is plotted in Figure 6. It is nearly sinusoidal. It becomes a maximum at $n = 3$ and 10 and a minimum when $n = 6$ and 13. Such a change is clearly due to coiling in the structure. The dipole moment values obtained from HF/6-311++G(d,p) and HF/aug-cc-pVDZ calculations show a similar variation with *n* for $(HP)_n$, $n = 1-6$ (see Figure 6). An analysis of the local structure of HP trimers in the helices reveals the crucial role played by the open book configuration in forming the helical motif. It is also clear that there are about six molecules per turn and the pitch of the helix is 11.8 Å at HF/6-31G* level and 11.48 Å at HF/6-311++G(d,p) level, as illustrated in Figure 7.

TABLE 6: O−H Stretching Frequencies and the Red Shifts Relative to the O−H Stretching Frequencies of the Monomer for Different $(HP)_n$ Clusters as Obtained from HF/6-31G* Calculations

	scaled frequencies (cm^{-1})		red shift (cm^{-1})	
cluster	ss	as	ss	as
1	3653 (3599)[a]	3655 (3608)[a]		
2-UU	3582 (3577)[a]	3603 (3582)[a]	73	53
2-UD	3582	3603	73	52
3A	3571−3574	3588−3605	82−86	52−69
4	3563−3573	3580−3603	82−93	53−76
5	3558−3575	3589−3602	79−96	53−65
6	3556−3572	3584−3602	82−98	53−71
7	3554−3572	3581−3602	83−101	53−74
8	3552−3571	3577−3602	84−103	53−78
9	3552−3575	3582−3602	79−103	53−72
10	3552−3573	3581−3602	81−103	53−74
11	3552−3572	3577−3602	83−103	53−77
12	3552−3572	3576−3602	83−103	53−79
13	3552−3571	3574−3602	84−103	53−80
14	3552−3572	3575−3602	83−103	53−79
15	3552−3572	3577−3602	83−103	53−78

[a] The corresponding experimental values[17] are given in brackets. ss: symmetric stretch. as: asymmetric stretch.

The equilibrium geometry of HP exhibits helical chirality. There are two conformations possible for the open book structure, and they differ from each other only by the sign of the dihedral angle. As a result, it is possible to obtain right- and left-handed helices in linear $(HP)_n$ clusters. The helical structure of $(HP)_n$ clusters, where $n = 13-15$, 22, and 28, are illustrated in Figure 8.

It is worth pointing out that Saha and Nangia[19] have reported helical water chains in aquapores of organic host lattices.

DFT and MP2 calculations yield qualitatively the same result as HF for $(HP)_n$, $n = 2$ and 3. **2-UD** is more stable than **2-UU**. For $n = 3$, the stability increases marginally in going from **3A** to **3B** to **3C**. The cyclic structure is comparable in stability to the linear, and the prism structure has the least stability. For both $n = 2$ and 3, BSSE corrected stabilization energies predicted by the MP2 method lie between the HF and DFT results. For $n = 4$, 5, and 6, all three methods predict the cyclic structure to be marginally more stable than the open linear (helical) structure. For $n = 7-15$, 22, and 28, only DFT calculations were carried out (in addition to the HF calculations

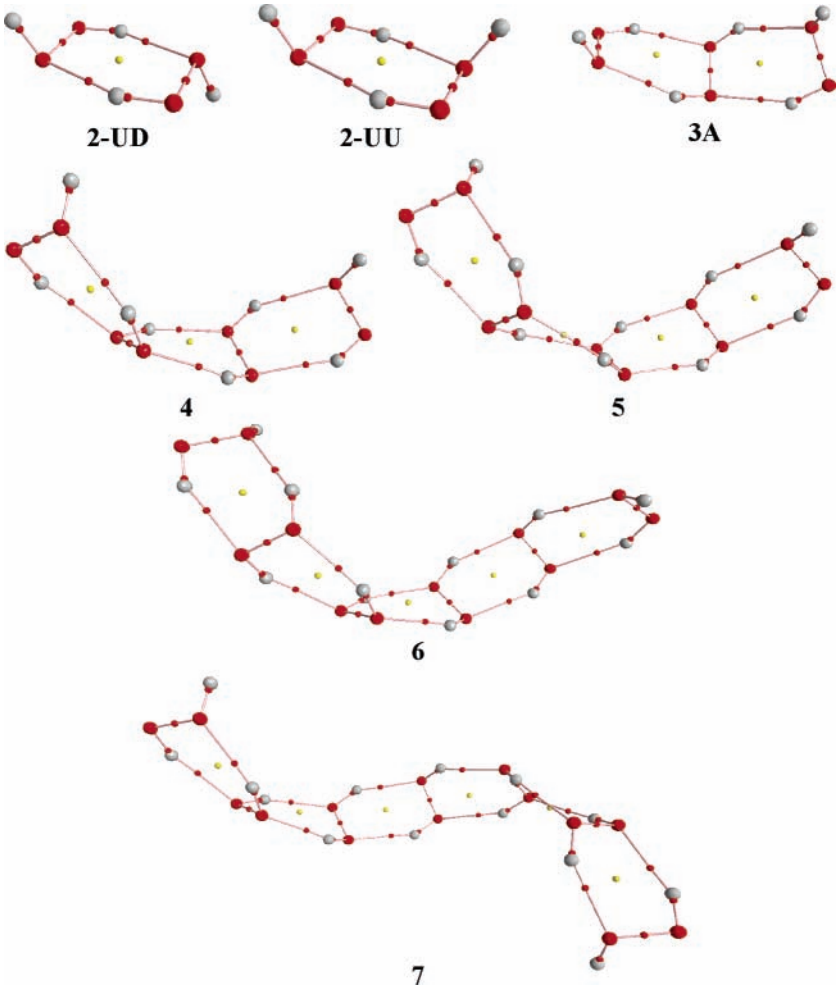

Figure 9. AIM features for $(HP)_n$ clusters, where $n = 2-7$, as obtained from HF/6-31G* calculations. The small red dots represent the bond critical points and the small yellow dots the ring critical points.

mentioned above), and they confirm the stability of the helical structures for $n \geq 10$. For $n = 4-9$, DFT calculations predicted structures that tend to coil, resulting invariably in the cage structures.

Vibrational frequencies for $(HP)_n$, $n = 2-15$, have been computed to ensure that all the structures presented in this paper do correspond to minima on the potential energy surface. The calculated red shifts in the frequencies of the O−H stretching mode in going from the monomer to the various oligomers are listed in Table 6, and they demonstrate clearly the presence of hydrogen-bonding interaction in all the clusters and its importance in the stabilization of the helical structures.

The presence of hydrogen bond critical points in $(HP)_n$, $n = 2-7$, clusters is shown as red dots in the electron density topographs in Figure 9. The value of electron density at the hydrogen bond critical point serves as an indicator of the nature and strength of the hydrogen-bonding interaction.[20] The calculated electron density values at the HBCPs range from 0.0199 to 0.0227 au, as illustrated in Table 7. The Laplacians of electron density at HBCPs are positive, confirming the formation of hydrogen bonds in the different clusters.

The molecular electrostatic potential map is quite useful in revealing the sites of hydrogen-bonding interaction in different clusters. The calculated MESP isosurfaces of some of the clusters are shown in Figure 10. The electrostatic potential minimum at the lone pairs of the oxygen atoms clearly dictates the direction of growth of the HP clusters.

TABLE 7: Electron Density and Laplacian of Electron Density for $(HP)_n$ Clusters, where $n = 2-7$ Obtained from HF/6-31G* Calculations

cluster	electron density (e/a_0^3)	Laplacian of electron density (e/a_0^5)
2-UU	0.021	0.019
2-UD	0.021	0.018
3A	0.021−0.022	0.019−0.020
4	0.020−0.022	0.018−0.020
5	0.020−0.022	0.018−0.020
6	0.020−0.023	0.018−0.020
7	0.020−0.023	0.018−0.020

IV. Concluding Remarks

Hydrogen-bonded clusters of $(HP)_n$, where $n = 1-15$, 22, and 28, have been investigated using HF, DFT(B3LYP), and MP2 levels of theory using the computationally manageable 6-31G* basis set. The geometrical parameters and stabilization energies for $(HP)_n$, $n = 1-6$, clusters have also been studied using 6-311++G(d,P), aug-cc-pVDZ, and aug-cc-pVTZ basis sets at the HF level. There is no significant change in the overall trends revealed by HF/6-31G* calculations. In all these clusters, each molecule of HP participates as a donor as well as an acceptor of hydrogen atoms. The HP clusters form nonplanar open book, cyclic, cage, and helical structures. In the helical structure, each HP trimer exhibits an open book conformation akin to that of the water hexamer. The strength of the hydrogen-bonding interaction is analyzed with the help of AIM topological parameters and red shifts in the OH stretching frequency. The

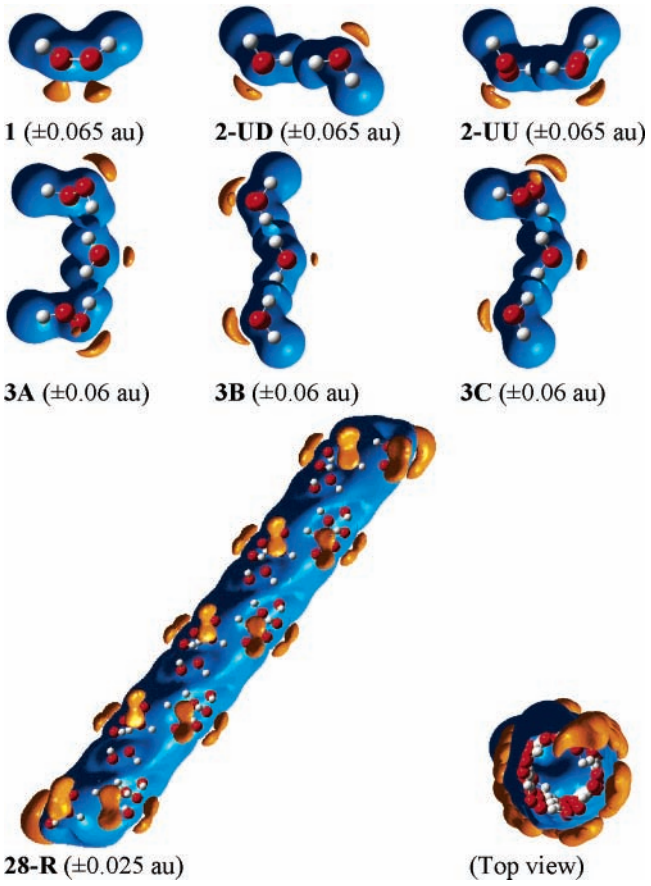

Figure 10. Molecular electrostatic potential maps generated for the HF/6-31G* optimized structures of hydrogen peroxide clusters. The isosurface value is given below the structures. Red spheres represent oxygen atoms and white spheres hydrogen atoms. Brown color represents the negative potential and blue the positive potential.

presence of lone pairs on the same side of the O−O−O−O plane is evident from the MESP features of the helical structures.

Acknowledgment. This study was supported in part by a grant from the Council of Scientific and Industrial Research, New Delhi.

References and Notes

(1) Jeffrey, G. A. *An Introduction to Hydrogen Bonding*; Oxford University Press: Oxford, 1997. Jeffrey, G. A.; Saenger, W. *Hydrogen Bonding in Biology and Chemistry*; Springer-Verlag: Berlin, 1991.

(2) Desiraju, G. R.; Steiner, T. *The Weak Hydrogen Bond*; Oxford University Press: Oxford, 1999. Scheiner, S. *Hydrogen bonding: A theoretical perspective*; Oxford University Press: Oxford, 1997.

(3) Maheshwary, S.; Patel, N.; Sathyamurthy, N.; Kulkarni, A. D.; Gadre, S. R. *J. Phys. Chem. A* **2001**, *105*, 10525. Keutsch, F. N.; Cruzan, J. D.; Saykally, R. J. *Chem. Rev.* **2003**, *103*, 2533.

(4) Liu, K.; Gregory, J. K.; Brown, M. G.; Carter, C.; Saykally, R. J.; Clary, D. C. *Nature (London)* **1996**, *381*, 501.

(5) Kim, J.; Kim, K. S. *J. Chem. Phys.* **1998**, *109*, 5886.

(6) Steinbach, C.; Andersson, P.; Kazimirski, J. K.; Buck, U.; Buch, V.; Beu, T. A. *J. Phys. Chem. A* **2004**, *108*, 6165. Steinbach, C.; Andersson, P.; Melzer, M.; Kazimirski, J. K.; Buck, U.; Buch, V. *Phys. Chem. Chem. Phys.* **2004**, *6*, 3320.

(7) Engdahl, A.; Nelander, B.; Karlstrom, G. *J. Phys. Chem. A* **2001**, *105*, 8393.

(8) Kulkarni, S. A.; Bartolotti, L. J.; Pathak, R. K. *Chem. Phys. Lett.* **2003**, *372*, 620.

(9) Frisch, M. J.; Trucks, G. W.; Schlegel, H. B.; Scuseria, G. E.; Robb, M. A.; Cheeseman, J. R.; Zakrzewski, V. G.; Montgomery, J. A., Jr.; Stratmann, R. E.; Burant, J. C.; Dapprich, S.; Millam, J. M.; Daniels, A. D.; Kudin, K. N.; Strain, M. C.; Farkas, O.; Tomasi, J.; Barone, V.; Cossi, M.; Cammi, R.; Mennucci, B.; Pomelli, C.; Adamo, C.; Clifford, S.; Ochterski, J.; Petersson, G. A.; Ayala, P. Y.; Cui, Q.; Morokuma, K.; Malick, D. K.; Rabuck, A. D.; Raghavachari, K.; Foresman, J. B.; Cioslowski, J.; Ortiz, J. V.; Stefanov, B. B.; Liu, G.; Liashenko, A.; Piskorz, P.; Komaromi, I.; Gomperts, R.; Martin, R. L.; Fox, D. J.; Keith, T.; Al-Laham, M. A.; Peng, C. Y.; Nanayakkara, A.; Gonzalez, C.; Challacombe, M.; Gill, P. M. W.; Johnson, B. G.; Chen, W.; Wong, M. W.; Andres, J. L.; Head-Gordon, M.; Replogle, E. S.; Pople, J. A. *Gaussian 98*, revision A.7; Gaussian, Inc.: Pittsburgh, PA, 1998.

(10) Parthasarathi, R.; Subramanian, V.; Sathyamurthy, N. *J. Phys. Chem. A* **2005**, *109*, 843.

(11) Elango, M.; Parthasarathi, R.; Subramanian, V.; Sathyamurthy, N. *J. Phys. Chem. A* **2005**, *109*, 8587.

(12) Boys, S. F.; Bernardi, F. *Mol. Phys.* **1970**, *19*, 553.

(13) Scott, A. P.; Radom, L. *J. Phys. Chem.* **1996**, *100*, 16502−16513. Fogarasi, G.; Pulay, P. *Annu. Rev. Phys. Chem.* **1984**, *35*, 191.

(14) Bader, R. F. W. *Atoms in Molecules: A Quantum Theory*; Clarendon Press: Oxford, U. K., 1990. Biegler-Konig, F.; Schonbohm, J.; Derdau, R.; Bayles, D.; Bader, R. F. W. *AIM 2000*, version 1; Bielefeld, Germany, 2000, www.aim2000.dc.

(15) Gadre, S. R.; Shirsat, R. N. *Electrostatics of Atoms and Molecules*; Universities Press: Hyderabad, India, 2000. Tomasi, J.; Mennucci, B.; Cammy, M. *Molecular Electrostatic Potentials: Concepts and Applications*; Murray, J. S., Sen, K. D., Eds.; Elsevier: Amsterdam, 1996. Gadre, S. R. Topography of Atomic and Molecular Scalar Fields. In *Computational Chemistry: Reviews of Current Trends*; Lesczynski, J., Ed.; World Scientific: Singapore, 2000; Vol. 4.

(16) Frisch, Æ.; Dennington, R. D., II; Keith, T. A.; Nielsen, A. B.; Holder, A. J. *GaussView 3.0*; Gaussian Inc.: Pittsburgh, PA, 2003.

(17) Koput, J. *J. Mol. Spectrosc.* **1986**, *115*, 438.

(18) Maeyama, T.; Mikami, N. *Phys. Chem. Chem. Phys.* **2004**, *6*, 2725.

(19) Saha, B. K.; Nangia, A. *Chem. Commun.* **2005**, 3024.

(20) Parthasarathi, R.; Subramanian, V.; Sathyamurthy, N. *J. Phys. Chem. A* **2006**, *110*, 3349.